

POTENTIAL APPLICATIONS OF PULSE ELECTRICAL DISCHARGES IN WATER ¹

P. Šunka², V. Babický, M. Člupek, M. Fuciman, P. Lukeš, M. Šimek,
J. Beneš*, B. Locke†, Z. Majcherová‡

*Institute of Plasma Physics, Academy of Sciences of the Czech Republic
Za Slovankou 3, 182 21, Prague 8, Czech Republic*

* *Charles university, First faculty of medicine, U nemocnice 2, Prague 2, Czech Republic*

† *Florida State University, College of Engineering, Tallahassee, Florida, USA*

‡ *Komenius University Bratislava, Slovak Republic*

Received 3 April 2003, accepted 23 February 2004

High voltage pulse electrical discharges in water solutions have been studied using different geometries of electrodes. It was demonstrated that discharges in all electrode configurations used (needle - plate, coaxial composite anode - tubular cathode and coaxial pinhole anode - tubular cathode) produce plasmas with very similar parameters. Plasma electron density depends strongly on the solution conductivity. Discharges in water have no counterpart in gas phase ones. The main chemically active specie produced by corona-like discharges is hydrogen peroxide, other species as H, O and OH radicals play a minor role. Degradation of phenol and decolorizing of organic dye "reactive blue 137" by OH radicals have been demonstrated. Corona-like discharges may find some applications in solution of environmental problems. At very high solution conductivity (5 - 20 mS/cm) multi-channel discharge with the composite anode generates strong acoustic waves. Focusing of the cylindrical pressure wave by parabolic metallic reflector and generation of spherically convergent wave has been demonstrated. Strong shock waves that lead to cavitation are formed at the focus region. Interaction of focused shock waves with cellular scale structures have been demonstrated. We believe that the focused shock waves will find some applications in medicine.

PACS: 52.35.Tc, 52.80.Wq, 82.33.Xj, 82.40.Fp

1 Introduction

Water is a polar liquid with a high electrical permittivity ($\epsilon_r = 80$) and a specific electrical conductivity σ . For a time τ of exposure of water to an electric field, when $\tau \ll \epsilon/\sigma$, the aqueous solution behaves as a dielectric medium, while for much longer times ($\tau \gg \epsilon/\sigma$) it behaves as a resistive medium. Deionized and degassed water ($\sigma < 1 \mu\text{S/cm}$, $\epsilon/\sigma > 7 \mu\text{s}$) has been commonly used as a dielectric in pulse forming lines for the generation of extremely high pulse

¹Presented at XIVth Symposium on Application of Plasma Processes, Liptovský Mikuláš (Slovakia), January 2003.

²E-mail address: sunka@ipp.cas.cz

power ($P > 1$ TW) with very short pulses ($T < 100$ ns) [1]. For a short line charging time ($t < 1$ μ s), the breakdown electric field E is ~ 500 kV/cm and the corresponding energy density $W = \epsilon E^2/2 \sim 1$ J/cm³. Breakdown in de-ionized water has been mostly studied to optimize design of pulse forming lines.

Different types of discharges utilizing high voltage and ground electrodes submerged in water or a high voltage electrode placed above the water surface with the ground placed in the water have been studied as possible methods for the degradation of organic compounds in solution. It has been demonstrated that a high voltage pulsed discharge with needle-plate electrodes geometry (a positive needle polarity), called a corona in analogy with gas discharges, produces chemically active species such as H, O, OH radicals and hydrogen peroxide H₂O₂ molecules [2-5]. The chemically active species can be used for the removal of low-level organic pollutants and microorganisms from water [6].

Understanding of corona-like electrical discharges in the liquid phase is much less developed than that for the gas phase due to less detailed knowledge of the ionization and collision events occurring in water solution. The difference between our understanding of the liquid phase and that of the gas phase discharge is not only due to the substantially higher density of the liquid leading to much higher collision frequency and lower mobility of charges but also due to a finite electrical conductivity σ of the liquid. Ions, present in the liquid with concentrations over 10^{18} cm⁻³ for $\sigma \sim 1$ mS/cm, strongly alter propagation of the streamer by compensating the space charge electric field on the streamer head.

It was found in experiments that an electric field of the order of 1 MV/cm is necessary to initiate the discharge in water. For a needle electrode totally insulated from the liquid, except at its tip, the pre-discharge electric field can be estimated as $E \sim U/r_c$, where U is the applied voltage and r_c is the radius of curvature of the needle tip [7]. Clearly, sharper needles generate the discharge at a lower applied voltage. However, sharp needles ($r_c \sim 0.05$ mm) are quickly eroded in the discharge, and at an average power of 100 W their lifetime is limited to 10 - 20 minutes. To overcome the limitation of the needle-plate electrodes we have developed metal electrodes coated by a thin porous ceramic layer [7]. The role of the ceramic layer is to enhance the electric field on the anode surface by concentration of the pre-discharge current in small open pores. Many discharge channels, distributed almost homogeneously on the electrode surface have been generated. The composite electrode can be made in various dimensions and geometrical configurations, enabling the construction of reactors that can operate at average power in the range of kW. Another electrode configuration used in liquid phase corona discharge is the "pinhole" geometry (also called a diaphragm discharge) whereby the high voltage and ground electrodes are separated by an insulating sheet with a small hole [8]. We have used the diaphragm discharge in coaxial electrode geometry, where the insulating sheet was placed directly on the surface of the inner high voltage anode.

Underwater spark discharge has been extensively studied in connection with the development of the so-called extra-corporeal shock wave lithotripsy, a noninvasive method for treatment of kidney stone disease [9]. High voltage/high current spark discharge between needle electrodes in water provides a point-like source of strong shock waves. If the discharge is situated in the focus of a semi-ellipsoidal metallic cavity, the wave energy is concentrated in the secondary focus. The interaction of the focused shock wave with the kidney stone positioned in the secondary focus results in crushing the stone into small particles that naturally leave the patient body. Formerly, we have developed a generator of focused shock waves with the spark discharge

that is used in clinical lithotripters [10]. The great success of the lithotripsy stimulated studies on the application of focused shock waves in other branches of medicine [11 and references there]. Much work has focused on the role of cavitations in cancer cell damage using commercial lithotripters [12] and special shock wave generators have been developed for these studies [13]. Recently we have developed a novel method for the generation of focused shock waves based on multi-channel discharge in water with a high conductivity [14]. In Section 2 we present results on the corona-like discharges in water using different electrode geometries, and in the next Section 3 we describe experiments on generation of focused shock waves by multi-channel electrical discharges in water.

2 Pulse corona-like discharges in water

2.1 Experimental setup

Measurements have been performed using three different types of reactors. The needle-plate and coaxial rod-tube electrode geometry reactors have been described elsewhere [7]. Briefly, for the needle-plate reactor the electrode system was immersed in a cylindrical glass vessel (ϕ 105x160 mm) with a needle-plate gap 28 mm. The HV tungsten needle anode was almost totally insulated with a Teflon tube from the surrounding water such that only a small conical tip of the anode (initial radius of curvature $\sim 70 \mu\text{m}$) was in direct contact with water. The coaxial reactor consisted of a stainless steel rod anode 6 mm in diameter surrounded by an external stainless steel tubular cathode of 30 mm in diameter. The 200 mm long anode was covered by a thin ($d_c = 0.2 - 0.3 \text{ mm}$) layer of porous ceramic (open porosity 2% - 5%, $\epsilon_{rc} \sim 8$) deposited on the rod surface by the technology of plasma spraying (composite anode).

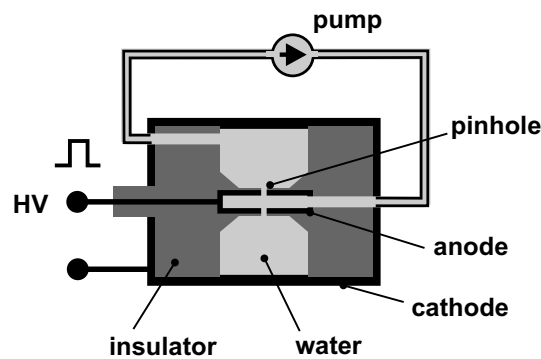


Fig. 1. Schematic of the "pinhole" reactor.

Preliminary experiments have also been conducted with a coaxial reactor with the pinhole discharge as schematically shown in Fig. 1. An inner tubular stainless steel anode of 12 mm in diameter is placed along the axis of a cylindrical cathode of 100 mm in diameter. The anode is covered by a polyethylene insulator and four holes of 0.7 mm in diameter are drilled in its thinnest 1mm central part. A treated liquid is pumped into the inner volume of the anode and flows into the inter-electrode volume through the holes. Computations of the spatial distribution of the pre-discharge electric fields revealed that all the mentioned electrode geometries create strongly

inhomogeneous electric fields with a very similar distribution [14] and generation of plasmas with similar parameters is to be expected. All the reactors were energized by the same pulse power supply. A storage capacitor 7, 14 or 21 nF was charged up to 30 kV, and by means of a rotating spark gap the voltage was switched to the reactor electrodes. Waveforms of the discharge voltage and current have been recorded by a digital oscilloscope using capacitive voltage divider and Rogowski coil, respectively. Time resolved emission spectroscopy in the range of 250-800 nm has been used for determination of plasma parameters. Production of the H_2O_2 and decolorizing of organic dyes in the discharges were measured by means of offline absorption spectroscopy. The solution conductivity was varied in the range of 0.1 - 1 mS/cm.

2.2 Experimental results

Most measurements have been conducted in the needle-plate reactor and in the coaxial reactor with the composite anode. The main results of the experiments can be concluded as follows: the discharge current increases with increasing solution conductivity.

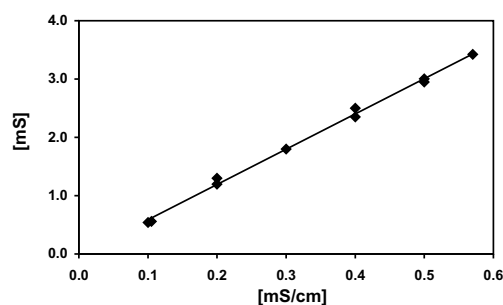


Fig. 2. Maximum conductance of the discharge (needle-plate reactor) $\Sigma = I/U$ at the applied voltage just below the sparking value versus the solution conductivity σ .

Fig. 2 demonstrates that the maximum conductance $\Sigma = U/I$ at the applied voltage U just below sparking is proportional to the solution conductivity σ . Simultaneously, the streamer channels become shorter due to a faster compensation of space charge electric field on the streamer head by ions. Two different phases have been observed in the temporal evolution of the streamer. During the first streamer-like phase the streamer propagates with a velocity of 10 km/s, reaching its maximum length of 10 - 15 mm. In the second arc-like phase the channel length remained constant in spite of the fact that the discharge current is still increasing.

The spectrum emitted by the discharge consists of the atomic hydrogen and oxygen spectral lines and of the OH radical band. Fig. 3 shows H_{α} line profile measured for different solution conductivity. It is apparent that the electron density in the discharge as determined from the H_{α} line profile increases from $2 \cdot 10^{17} \text{ cm}^{-3}$ for $\sigma = 0.1 \text{ mS/cm}$ to above 10^{19} cm^{-3} for $\sigma = 1 \text{ mS/cm}$. Fig. 4 demonstrates that the main chemically active product of the discharge is hydrogen peroxide H_2O_2 . The time dependence of the phenol removal (time expressed in the total energy deposited in the discharge) is plotted in the figure for three different conditions. Phenol in an amount of 1 mmol/l was dissolved in distilled water and NaCl was added to adjust the solution conductivity to 0.11 mS/cm. Line (1) demonstrates the negligible role of electrolysis in phenol degradation.

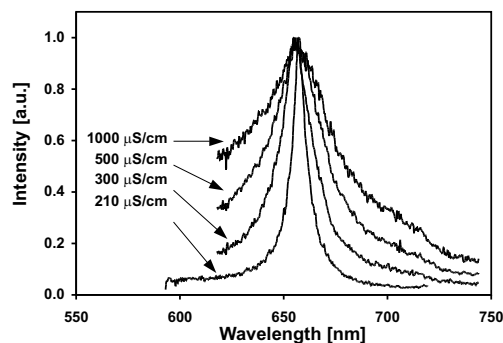


Fig. 3. H_{α} line profile at the initial phase of the discharge ($t = 450$ ns) for different solution conductivity demonstrating growth of the electron density n_e with the increasing solution conductivity σ .

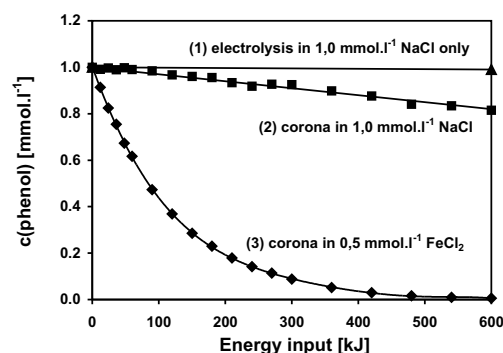


Fig. 4. Phenol removal (1 mmol/l) for (1) electrolysis only, (2) corona discharge in 1 mmol/l NaCl, (3) corona discharge in 0.5 mmol/l $FeCl_2$, needle-plate reactor, initial $\sigma=0.11$ mS/cm, $U=26$ kV/50 Hz.

In these experiments the applied voltage was slightly below the inception value and therefore, no discharge was generated. Line (2) corresponds to the corona discharge in the same solution at the applied voltage near the sparking value. The relatively small amount of phenol degradation is apparently caused by the oxidative action of OH radicals produced by the discharge. Line (3) demonstrates that a significant amount of H_2O_2 is produced by the discharge. Through addition of 0.5 mmol/l of $FeCl_2$ to the solution containing phenol in distilled water, the hydrogen peroxide was decomposed to OH radicals according to the Fenton's reaction



This reaction results in an increased concentration of OH radicals and thus in much faster phenol degradation. Since H_2O_2 is the dominant chemically active product of the discharge, its production was studied in more detail using the needle-plate reactor. In these experiments the following conditions were varied, the pH of the solution (3 - 11), the value of the storage capacitor (1 - 10 nF - different pulse duration), and the applied voltage from slightly above the inception value up to sparking. Surprisingly, the efficiency of H_2O_2 production was constant under all experimental conditions. The concentration of H_2O_2 initially increased with time and became saturated

at long time. However, the rate of production of H_2O_2 strongly decreased with the increasing solution conductivity.

To demonstrate the close similarity of the plasma parameters for the different electrode configurations, we measured H_2O_2 production in all three reactors with solution conductivities of 0.3 mS/cm. Phenol in an amount of 1 mmol/l was added into the solutions to exclude effect of the OH radicals produced in the discharge on H_2O_2 . The results of these experiments presented in Fig. 5 demonstrate very similar efficiencies of the H_2O_2 production. The slightly lower efficiencies measured for the composite rod-tube and pinhole reactors may be caused by energy losses during the pre-discharge phase when the discharge current started with some delay after the voltage pulse.

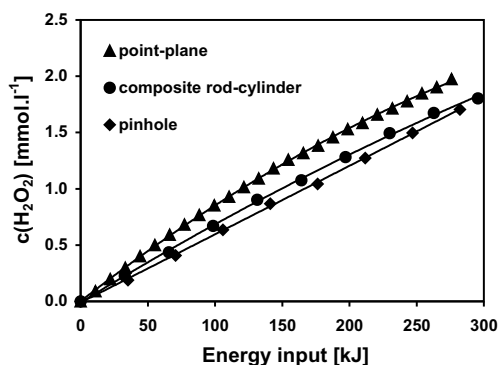


Fig. 5. Production of H_2O_2 in reactors with different electrode configurations. Solution conductivity $\sigma=0.3$ mS/cm, 1 mmol/l of phenol was added into the solution.

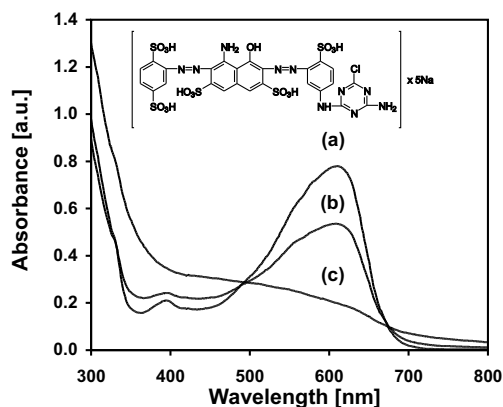


Fig. 6. Absorbance of the "reactive blue 137". (a) non-treated solution, (b) solution treated 30 minutes by the discharge, (c) treatment time 5 minutes, Fe ions added into the solution. Structure of the dye molecule is inserted.

The pinhole reactor has been used for preliminary tests on decolorizing of the organic dye "reactive blue 137". The dye in an amount of 50 mg/l was dissolved in water with a conductivity of 1 mS/cm. The solution was pumped into the inner volume of the anode and circulated through

the reactor. The solution temperature was maintained at 15°C. The pulse power supply with a condenser of 14 nF was used. The sample absorbance taken at 5 minutes intervals was measured in the spectral range 300 - 800 nm. The results are presented in Fig. 6. The curve (a) corresponds to the non-treated solution. The curve (b) exhibits a partial degradation of the dye caused by OH radicals generated after 30 minutes of discharge operation. No ferrous ions were added to the solution. The curve (c) shows that the addition of ferrous ions to the solution results in full decolorizing of the dye after 5 minutes of exposure to the discharge. This result once more demonstrates the decisive role of hydrogen peroxide in the process.

3 Generation of focused shock waves in water

3.1 Experimental setup

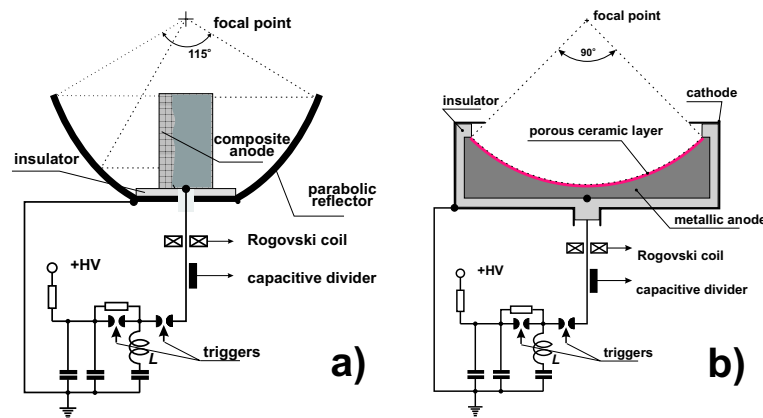


Fig. 7. Schematic diagram of generator of cylindrical pressure wave focused by a parabolic reflector (a) and generator producing spherically convergent pressure wave (b).

Two versions of the focused shock waves generators have been developed. In the first version (Fig. 7a) a cylindrical pressure wave is produced by a multi-channel discharge at a cylindrical metallic anode covered by a thin layer of porous ceramics (composite anode). In highly conducting water a large number of short discharge channels is created and these channels are distributed almost homogeneously on the anode surface. Each discharge channel expands and creates a semi-spherical pressure wave, and by superposition of all the waves a cylindrical wave propagating from the anode is formed. The cylindrical pressure wave is focused by a metallic parabolic reflector, and near the focus this pressure wave is transformed into a strong shock wave. Shape of the inner reflector surface is given by the equation

$$y = 250 - [250(250 - 2x)]^{1/2}, x \in < 60; 115 >, y \in < 70; 180 >$$

The second version of the generator produces spherically convergent pressure waves. The same type of the multi-channel discharge between a composite anode in the form of a part of a spherical cavity ($R = 150$ mm, aperture diameter 200 mm) and a ring shaped cathode (inner

diameter of 160 mm situated 25 mm from the anode aperture) was used - Fig. 7b. The solution conductivity was varied in the range of 5 - 20 mS/cm. The generators have been placed in a tank where the conductive liquid was separated from the experimental volume containing distilled water by an acoustically transparent membrane. The pulse power supply consisted of three condensers $0.5 \mu\text{F}$ each, charged up to 30 kV and two triggered spark gaps. This arrangement enables us to produce either a single shock or two subsequent discharges with a variable time delay. The discharge voltage and current was measured in the same manner as in the corona discharges. Schlieren photography was used for visualization of the pressure field in the focal region. Calibrated pressure sensors (PVDF produced by the French company PIEZOTECH S.A.) with a temporal resolution of 50 ns and with an active area of 1, 4 and 9 mm^2 have been used for measurements of waveforms of the shocks in the focal region. The sensitivity of the probes, as measured by the producer, is in the range of 22.5 - 24.5 pC/N.

3.2 Experimental results

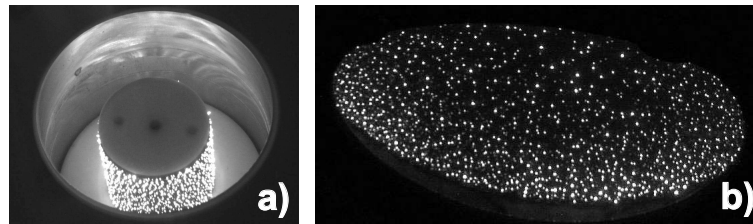


Fig. 8. Photographs of a single shot discharge at cylindrical (a) and spherical (b) composite anodes. $U = 28 \text{ kV}$, $C = 1 \mu\text{F}$, $\sigma = 12 \text{ mS/cm}$.

Photographs of a single shot discharge at the cylindrical and at the spherical composite anodes are shown in Fig 8 a, and b, respectively. The pictures ($U = 28 \text{ kV}$, $C = 1 \mu\text{F}$, solution conductivity $\sigma = 12 \text{ mS/cm}$) demonstrate the formation of a large number of channels with a high surface density to form cylindrical and spherical pressure waves. The waveforms of the shock waves as measured at the focus of the parabolic reflector for different applied voltages are shown in Fig. 9. A sensor with an active area of 4 mm^2 was used.

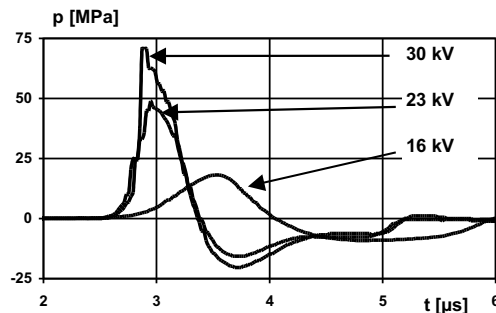


Fig. 9. Waveforms of the shock wave measured at the focus for different applied voltage. Generator with cylindrical anode and parabolic reflector.

At the applied voltage of $U=16$ kV the initial pressure wave was not strong enough to be fully transformed to shock wave at the focal region as occurred at the higher voltages of 23 kV and 30 kV. The signal on the pressure probe appeared $147 \mu\text{s}$ after the discharge started. Thus, the shock front propagates with the speed of sound in water (1500 m/s). Cavitation bubbles were visible at the focal region. Transverse profiles of the pressure wave at the focal plane of both generators are shown in Fig. 10. Due to very sharp focusing of the wave the pressure

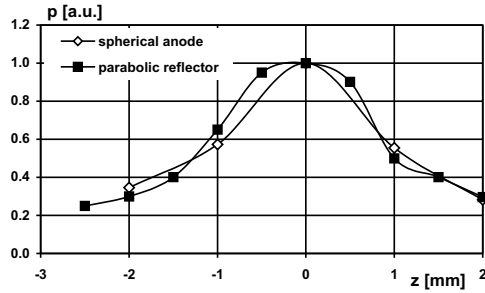


Fig. 10. Transverse profiles of the pressure waves at the focus.

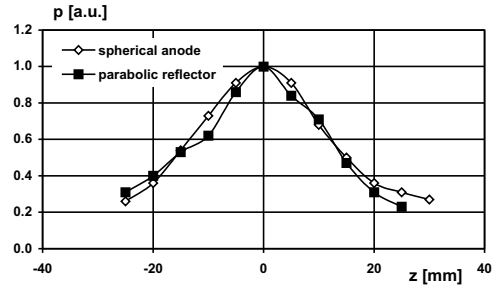


Fig. 11. Longitudinal pressure profiles at the focal region.

amplitude can be correctly measured only by a sensor with the smallest active area 1×1 mm. In this case the shock wave amplitude increased almost proportionally to the applied voltage reaching 90 MPa at $U = 25$ kV. These high pressure shock waves damaged the sensor after several tens of shots. The longitudinal pressure profiles at the focal region are shown in Fig. 11. Analysis of schlieren photographs taken at different phases of the wave propagation reveal that in spite of the very high shock amplitudes measured by the pressure probe at the focus, the waves propagate almost in agreement with geometrical acoustic. Figs. 10. and 11. demonstrate that both the generators produce almost identical shock waves. Such similarity can be expected due to the similar wave convergent angles. The dimensions of the focal volumes (full width at a half maximum - FWHM) are $\phi 2,5 \times 32$ mm for both the generators. Interaction of the focused shock waves (single discharge) with cellular scale structures has been tested. Cellular damage induced by the shock waves was demonstrated on hemolysis of human erythrocytes.

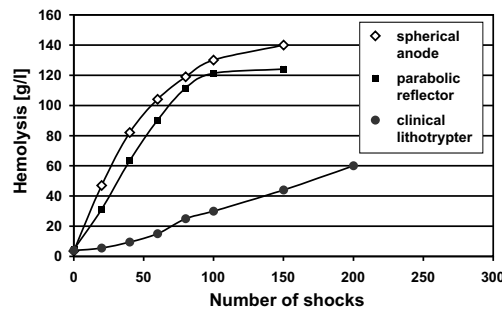


Fig. 12. Hemolysis of human erythrocytes exposed to shock waves produced by both the generators and comparison with the generator used in clinical lithotripsy.

Polypropylene vials of 0.6 ml volume (outside dimensions ϕ 6 x 25 mm) were filled with native human blood, placed to the focal region and exposed to different numbers of shock waves. The vials were oriented perpendicularly to the system axis. In addition to the present generators we also used an electro-hydraulic generator with a spark discharge that is used for clinical lithotripsy. Experimental results are shown in Fig. 12. In the case of the clinical generator the hemolysis increased proportionally to the number of shocks reaching 60 g/l (roughly 1/3) after 200 shocks, whereas the new generators caused hemolysis 80 g/l after 30 shocks and 140 g/l (almost total) after 150 shocks. A simple method to assess the mechanical effects of the focused shock waves is to study the interaction with fresh potatoes that have a high water content. It is known that mechanical damage to a potato results in a color change of the damaged volume. We exposed a 2 cm thick slab of a fresh potato to the shock waves. The slab was placed to the focal region perpendicularly to the system axis and exposed to 50 shocks at 30 kV. The potato was then cut along the axis and after several hours the damaged region became dark as shown in Fig. 13. The dark damaged region corresponds to the geometry of the used reflector. A similar experiment has been conducted with a 6 cm thick slab of potato exposed only by 10 shock waves. Fig. 14 demonstrates that only the focal region of the potato has been damaged and no damage was seen between the potato surface and the focal region.

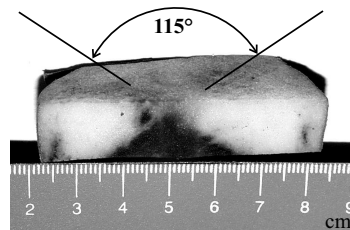


Fig. 13. Photograph of slab of potato exposed by 50 shock waves.

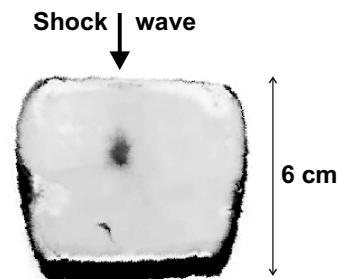


Fig. 14. 6 cm thick slab of potato exposed by 10 shock waves.

4 Conclusions

High voltage pulse electrical discharges in water solutions have been studied using different electrode geometries. It was demonstrated that the discharges in all electrode configurations used (needle-plate, coaxial composite anode - tubular cathode and coaxial pinhole anode - tubular cathode) produce plasmas with very similar parameters. The plasma electron density depends strongly on the solution conductivity reaching over 10^{17} cm^{-3} at a conductivity of 0.05 mS/cm and increasing to over 10^{19} cm^{-3} for $\sigma = 1 \text{ mS/cm}$. Such discharges have no counterpart in the gas phase. The main chemically active species produced by corona-like discharges in water is hydrogen peroxide, and other species such as H, O and OH radicals play a minor role. The degradation of phenol and decolorization of the organic dye "reactive blue 137" by OH radicals have been demonstrated. Corona-like discharges may find some applications in solution of environ-

mental problems. At very high solution conductivity (5 - 20 mS/cm) the multi-channel discharge on the composite anode generates strong acoustic waves. Focusing of the cylindrical pressure wave by parabolic metallic reflector and generation of spherically convergent waves have been demonstrated. Strong shock waves that lead to cavitation are formed at the focus region. We believe that the focused shock waves will find some applications in medicine.

Acknowledgement: This work was supported by the Academy of Sciences of the Czech Republic under the contract No. S2043004, by the Grant Agency of the Czech Republic, Contract No. 202/02/1026 and by the Ministry of Education, Youth and Sports of the Czech Republic under the Contract No. ME 472 - KONTAKT.

References

- [1] Allan J. Toepfer: in *Advances in Electronics and Electron Physics*. (Ed. L. Marton, C. Marton) Academic, New York 1980, Vol. 53, p.1.
- [2] B. Sun, M. Sato, J. S. Clements: *J. Electrostat.* **39** (1997) 189
- [3] A. A. Joshi, B. R. Locke, P. Arce, W. C. Finney: *Journal of Hazardous Materials* **10** (1995) 3
- [4] W. F. L. M. Hoeben, E. M. van Veldhuizen, W. R. Rutgers, G. M. W. Koersen: *J. Phys. D* **32** (1999) 133
- [5] P. Šunka, V. Babický, M. Člupek, P. Lukeš, M. Šimek, J. Schmidt, M. Černák: *Plasma Sources Sci. Technol.* **8** (1999) 258
- [6] B. Sun, M. Sato, J. S. Clements: *J. Phys. D* **32** (1999) 1908
- [7] P. Šunka, V. Babický, M. Člupek, M. Černák: in *Proc. ESCAMPIG 96, Poprad, Slovakia August 27-30 1996*. (Ed. Lukáš, Košinár, Skalný) Bratislava, Vol 20E, Part A, p. 125
- [8] E. M. Drobishevskii, Yu. A. Dunayev, S. I. Rozov: *Zh. Tekh. Fiz.* **43** (1973) 1217, in Russian
- [9] M. Burlion, P. Dancer, F. Lacoste: *Rev. Sci. Instrum.* **65** (1994) 2356
- [10] P. Šunka, V. Babický, M. Člupek, Č. Štuka: in *Proc. 19th Int. Symp. On Shock Waves, Marseille July 26-30 1993*, ed. by R. Brun, L. Z. Dumitresku; Springer-Verlag Berlin-Heidelberg 1995, Vol. III, p.255
- [11] A. J. Coleman, J. E. Sounders: *Ultrasonics* **31** (1993) 75
- [12] F. Prat, J. Y. Chapelon, T. Ponchon, F. Abou El Fadil, G. Theilliere, D. Pansu, F. Berger, D. Cathinghol: in *Proc. 18th Int. Symp. on Shock Waves, Sendai 1991*, ed. by K. Takayama, Vol. II, p.1163
- [13] F. Prat, A. Arefiev: in *Proceedings of the 19th Int. Symp. on Shock Waves, Marseille 1993*, ed. by R. Brun, L. Z. Dumitresku; Springer-Verlag, Berlin, 1995, Vol. III, p. 21.
- [14] P. Šunka: *Physics of Plasmas* **8** (2001) 2587